

Contents lists available at ScienceDirect

Chemical Engineering Journal

journal homepage: www.elsevier.com/locate/cej





Highly stable CsPbBr₃ quantum dots by silica-coating and ligand modification for white light-emitting diodes and visible light communication

Xianwen Li^a, Wensi Cai^a, Hongling Guan^a, Shuangyi Zhao^a, Siliang Cao^a, Chen Chen^{b,*}, Min Liu^b, Zhigang Zang^{a,*}

ARTICLE INFO

Keywords:
CsPbBr₃ quantum dots
DDAB capped
Silica-coated
Warm white light-emitting diodes
Visible light communication

ABSTRACT

Owing to their superior optical and electronic properties, all inorganic metal halide CsPbX₃ (X = Cl, Br, and I) perovskite quantum dots (QDs) are regarded as excellent candidates for various optoelectronic applications. However, the instability of such materials greatly hampers their practical applications. In this work, silica-coated didodecyldimethylammonium bromide (DDAB) capped CsPbBr₃ QDs are prepared via a facile method at room temperature. The as-prepared DDAB-CsPbBr₃/SiO₂ QDs composites demonstrate an effectively improved photoluminescence quantum yield (PLQY) and stability against ethanol and heat. Moreover, the green DDAB-CsPbBr₃/SiO₂ QDs composites and red InAgZnS QDs are applied as color-converting layers on a blue LED chip for warm white light-emitting diodes (WLEDs). Such WLEDs exhibit an excellent luminescent performance with a color rendering index (CRI) of 88, a color coordinate of (0.41, 0.38), a correlated color temperature (CCT) of 3209 K, and a high power efficiency of 63.4 lm W⁻¹. Besides, such WLEDs are used for visible light communication (VLC), exhibiting a typical low-pass frequency response, with a corresponding -3 dB bandwidth of about 1.5 MHz. By applying orthogonal frequency division multiplexing (OFDM) with a bit loading, a maximum achievable rate of the VLC system reaches 5.9 Mbps, which is almost four times of their measured -3 dB bandwidth. These results demonstrate the potential of prepared DDAB-CsPbBr₃/SiO₂ QDs composites not only in high-performance WLEDs, but also as an excitation light source to achieve VLC.

1. Introduction

Recently, all-inorganic metal halide CsPbX $_3$ (X = Cl, Br, and I) perovskite quantum dots (QDs) have been regarded as one of the most promising materials for lighting and display applications, owing to their high absorption coefficient, tunable emission band-gap [1–4], high photoluminescence quantum yield (PLQY) and low-cost [5–15]. Especially, CsPbBr $_3$ QDs have a higher PLQY and a smaller FWHM compared to CsPbCl $_3$ QDs and CsPbI $_3$ QDs, which is due to the less formation of deep defect states in Br based perovskites [13]. The so-called Helmholtz-Kohlrausch effect states that high saturation of colors caused by small FWHM, which ensure a high CRI of WLEDs based on CsPbBr $_3$ [14]. Therefore, CsPbBr $_3$ QDs have been incorporated into warm white lightemitting diodes (WLEDs) to act as luminescent components and to improve the performance of white emission [7,16,17]. Unfortunately,

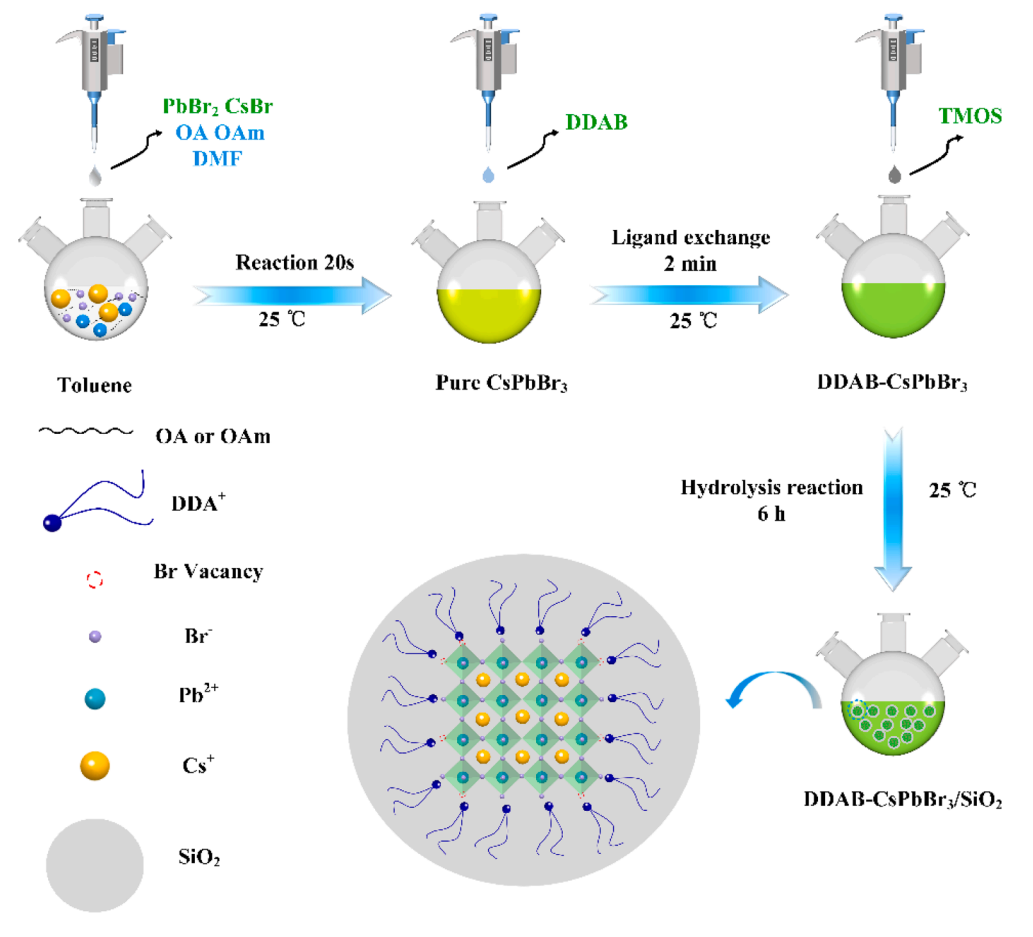
although the reported CsPbBr3 QDs have a high PLQY due to its defect-tolerant nature, the ability of such defect-tolerant is limited, and QDs were generally vulnerable to moisture, oxygen, heat and light [18–20], limiting their practical applications. In recent years, various strategies have been proposed to improve the stability of CsPbBr3 QDs through chemical and physical methods [21–25], i.e., the widely studied ligands modification [25–33]. Oleylamine (OAm) and oleic acid (OA) are traditional ligands used to synthesize CsPbBr3 QDs, however, the obtained QDs suffer issues of low PLQY and poor stability due to the ligands loss. To solve this, Pan et al. realized highly efficient perovskite-quantum-dot light-emitting diodes by using stable films of CsPbX3 QDs capped with a halide ion pair [25]. Zhang et al. used octylphosphonic acid (OPA) to replace OAm and OA ligands, and successfully synthesize high performance CsPbBr3 QDs [26]. Imran et al. proposed a post-processing ligand exchange strategy involving the displacement of

E-mail addresses: c.chen@cqu.edu.cn (C. Chen), zangzg@cqu.edu.cn (Z. Zang).

a Key Laboratory of Optoelectronic Technology & Systems (Ministry of Education), Chongqing University, Chongqing 400044, PR China

^b School of Microelectronics and Communication Engineering, Chongqing University, Chongqing 400044, PR China

^{*} Corresponding authors.



Scheme 1. A schematic of reaction process showing the formation of DDAB-CsPbBr₃/SiO₂ QDs composites.

both cationic and anionic ligands on native model systems of CsPbBr₃ QDs, exhibiting both an excellent heat stability over 3 weeks and a nearunity PLQY [27]. Our group reported an effective ligand-modification method using 2-hexyldecanoic acid (DA) to synthesize CsPbBr₃ QDs, resulting in an improved PLQY and a high stability over two months [28]. Zeng et al. synthesized CsPbBr₃ QDs with only dodecylbenzene sulfonic acid (DBSA), achieving a PLQY higher than 90%, a high flux photo irradiation, and maintaining a stable performance even after being stored in air for more than five months [29]. However, the abovementioned synthesis processes are quite complex and require high temperature treatments, which are not conducive to commercial applications.

Alternatively, stable perovskite QDs could be achieved by coating with oxide materials, such as SiO_2 [10,34–39], TiO_2 and Al_2O_3 [40,41]. Among them, SiO2 is a good choice because of its low-cost, high controllability and easy integration with other applications [42-44]. Furthermore, the whole synthesis process is simple and can be done entirely at room temperature, making it quite suitable for commercial applications. Based on this, Song et al. reported the mono-dispersed perovskite QDs@SiO2 composites synthesized by low temperature method [44]. Zhang et al. reported a facile one-pot approach to synthesize CsPbBr3@SiO2 core-shell nanoparticles, showing an enhanced long-term stability both in humid air and against ultrasonication in water [45]. Our group also introduced a facile strategy for making monodispersed SiO₂ coated Mn²⁺ doped CsPbX₃ QDs (X = Br, Cl), showing an improved thermostability and water resistance [46]. However, since the reaction processes require the adding of water or catalyst, a decomposition of QDs by water might occur even before the generation of oxides, and hence causing a low PLQY in QDs prepared using the above-mentioned methods. To solve it, it is of great importance to develop a benign strategy to uniformly encapsulate the CsPbBr₃ QDs.

In this work, we report a facile strategy to synthesize DDAB-CsPbBr₃/ SiO_2 QDs composites at room temperature in air. As shown in Scheme 1, we employ didodecyldimethylammonium bromide (DDAB) as surface ligands to exchange OAm and OA ligands for modification of CsPbBr₃ QDs, and then coat QDs with SiO2 by adding tetramethoxysilane (TMOS), resulting in a high PLQY of 82% for the obtained DDAB-CsPbBr₃/SiO₂ QDs composites as well as a substantially improved stability against heat and polar solvent. Finally, high performance WLEDs and visible light communication (VLC) systems based on such encapsulated CsPbBr₃ ODs are realized. The fabricated WLEDs exhibit an excellent luminescent performance with a color rendering index (CRI) of 88, a color coordinate of (0.41, 0.38), a correlated color temperature (CCT) of 3209 K, and a high power efficiency of 63.4 lm W^{-1} . By applying orthogonal frequency division multiplexing (OFDM) with a bit loading, the maximum achievable rate of the VLC system reaches 5.9 Mbps, which is almost four times of their measured -3 dB bandwidth.

2. Experimental

2.1. Materials

Cesium Bromide (CsBr, 99.99%, from Xi'an Polymer Light Technology Cor.), lead (II) bromide (PbBr $_2$, 99.99%, from Xi'an Polymer-Light Technology Cor.), oleic acid (OA, 90%, from Aladdin reagent), oleylamine (OAm, 80–90%, from Aladdin reagent), N, N-dimethylformamide (DMF, 99.9% from Sigma-Aldrich), didodecyldimethylammonium bromide (DDAB, 99.8% from Aldrich reagent), Tetramethoxysilane (TMOS, 99.5% from Aldrich reagent), toluene (anhydrous, 99.5%).

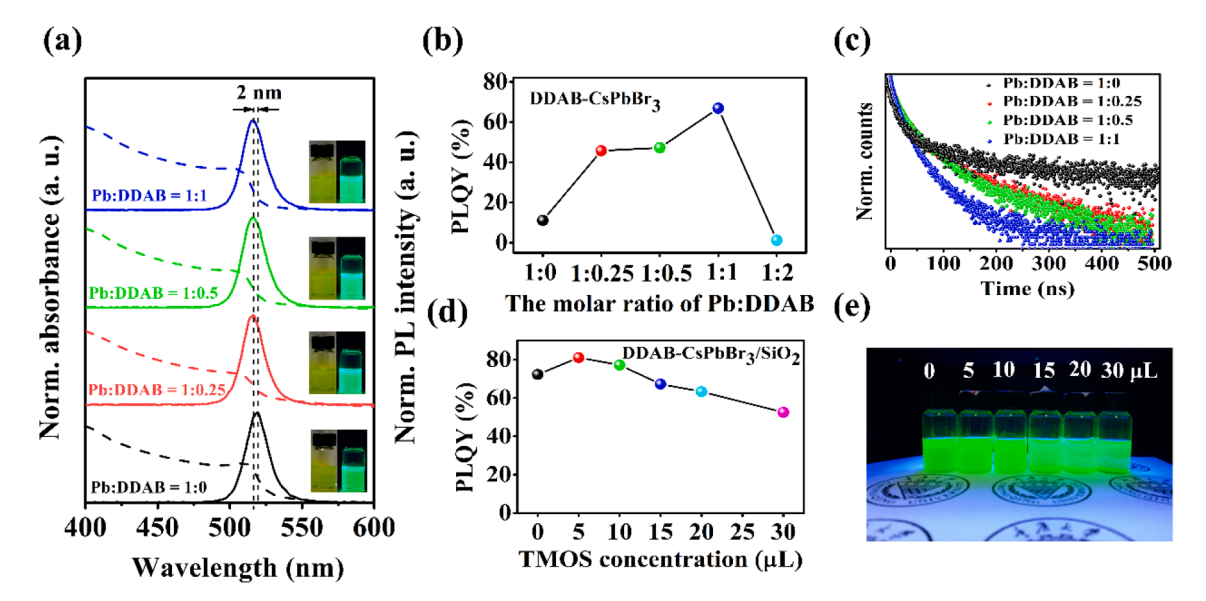


Fig. 1. (a) Absorption spectra and PL spectra of DDAB-CsPbBr₃ QDs with different molar ratios of Pb:DDAB. (The insets show pictures of DDAB-CsPbBr₃ QDs without/with UV light) (b) PLQY and (c) PL decay curves of DDAB-CsPbBr₃ QDs with different molar ratios of Pb: DDAB., (d) PLQY values as a function of TMOS concentration. (e) Photographs of DDAB-CsPbBr₃/SiO₂ QDs composites with different amount of TMOS (0, 5, 10, 15, 20 and 30 μL) under UV light.

2.2. Synthesis of pure CsPbBr₃ QDs and DDAB-CsPbBr₃ QDs

The precursor solution was obtained by first dissolving PbBr $_2$ (0.4 mmol) and CsBr (0.4 mmol) in DMF (12 mL), followed by the adding of OAm (0.2 mL) and OA (0.8 mL) into the mixture. Then, it was stirred for half an hour to obtain a clear solution. After that, 0.5 mL precursor solution was quickly added into 10 mL toluene under vigorous stirring at 1500 rpm for 20 s to synthesize pure CsPbBr $_3$ QDs. DDAB-CsPbBr $_3$ QDs were synthesized by adding DDAB into obtained fresh pure CsPbBr $_3$ QDs under vigorous stirring at 1500 rpm for 2 min to achieve ligands exchange.

2.3. Synthesis of DDAB-CsPbBr3/SiO2 QDs composites

Solutions containing DDAB-CsPbBr $_3$ QDs were prepared using the method mentioned in 2.2. Then, TMOS was added into 10 mL of such solutions under a vigorous stirring at 300 rpm for 6 h to grow DDAB-CsPbBr $_3$ /SiO $_2$ QDs composites.

2.4. Fabrication of WLEDs

10~mg polymethyl methacrylate (PMMA) and 20~mg DDAB-CsPbBr $_3/$ SiO $_2$ QDs composites (1:2) (Pb:DDAB =1:1) were dissolved in15mL toluene and stirred for 1~h. Similarly, 10~mg PMMA and 20~mg AgInZnS QDs were dissolved in 15~mL toluene and stirred for 24~h. To fabricate WLEDs, the above obtained two solutions were dropped on a commercially available blue chip and then annealed at $50~^{\circ}\mathrm{C}$ for 30~min.

2.5. Measurements of the VLC system

The electrical AC signal is generated by an arbitrary waveform generator (AWGRigol DG4102), which is further combined with a 3.0 V DC bias via a bias-T (Mini-Circuits Bias-Tee ZFBT-6 GW +). The combined signal is then used to drive WLEDs with DDAB-CsPbBr $_3$ /SiO $_2$ to generate white light. At the receiver side, a photodetector (PD) (DH-GDT-D020V) with a -3 dB bandwidth of 10 MHz is used to convert the optical signal into an electrical signal. The resultant electrical signal is further sampled by a digital storage oscilloscope (DSO) (LeCroy Wave-Surfer 432) and the obtained digital signals are processed offline via MATLAB.

2.6. Characterizations

The X-ray diffraction (XRD) patterns of all samples were measured by a Cu Ka radiation using XRD-6100, (SHIMADZU, Japan). Fourier Transform Infrared (FTIR) spectra were performed using KBr tablets and a Nicolet iS50 FT-IR Spectrometer (Thermo Fisher Scientific, Waltham, MA, USA). X-ray photoelectron spectroscopy (XPS) spectra were obtained using an ESCA Lab220I-XL. The TEM images were recorded by a transmission electron microscope (Libra 200 FE, Zeiss, Germany). Absorption spectra were enforced by a UV-vis spectrophotometer (UV-vis: UV-2100, SHIMADZU, Japan). Photoluminescence spectroscopy was implemented by a fluorescence spectrophotometer (Agilent Cary Eclipse, Australia), using a Xe lamp as an excitation source with optical filters. Time-resolved fluorescence spectra were performed by a GL-3300 fluorescence lifetime spectrofluorometer, (Photon Technology International Inc, USA), PL QY was measured using a FLSP920a spectrofluorometer (Edinburgh Instruments Ltd., United Kingdom). The optical parameters of the fabricated WLEDs were performed using a spectrograph of PR670 with an analyzer system. All tests were done at room temperature.

3. Results and discussion

To explore the influence of DDAB on the optical performance of CsPbBr₃ QDs, photoluminescence (PL) and absorption spectra of DDAB-CsPbBr₃ QDs synthesized using different molar ratios of Pb:DDAB were performed. Fig. 1a shows that the increase of DDAB amount leads to a blue-shift of both PL emission peak position (from 517 to 515 nm) and absorption peak position (from 512 to 508 nm), which might be due to the adsorption of DDAB on the surface of QDs and the formation of slightly smaller particles. This is consistent with the photograph under the UV light (the inset of Fig. 1a). Figure S1a shows the optical properties upon the excess of DDAB treated CsPbBr3 QDs, in which the PL peak is located at 515 nm while the absorption peak is difficult to observe, suggesting that the excess of DDAB ligand might lead to a degradation of the CsPbBr3 QDs (Figure S1b). Also, as shown in Fig. 1b, the increase of Pb: DDAB molar of ratio to 1:1 causes the significantly increase of PLQY from 11.02 to 72.75%, which might be due to the exchange of OA and OAm by DDAB on the QDs surface. This exchange process might contribute to two functions in QDs. On one hand, similar to what were reported previously [25], the exchange process could

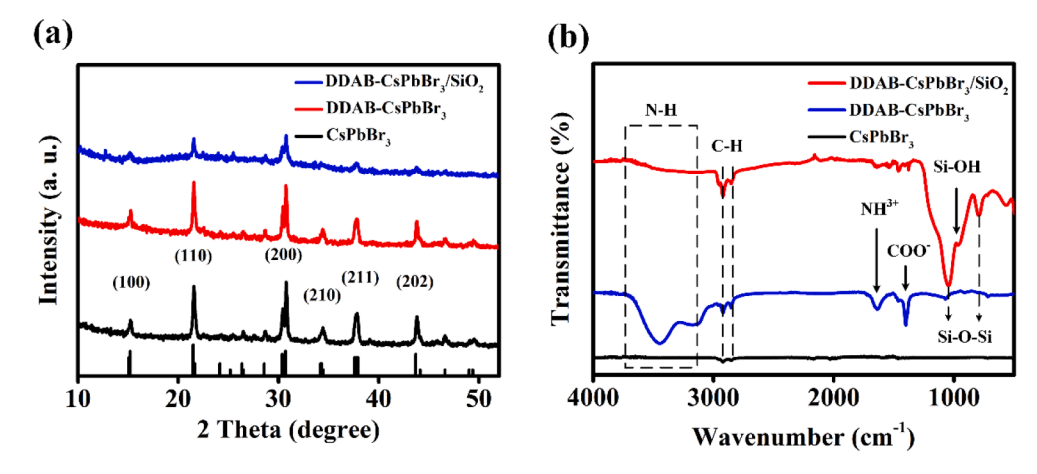


Fig. 2. (a) XRD patterns and (b) FTIR of CsPbBr3 QDs, DDAB-CsPbBr3 QDs and DDAB-CsPbBr3/SiO2 QDs composites.

enhance the affinity of Br $^-$ ions to Pb $^{2+}$ or Cs $^+$ on the surface of QDs, on the other hand, the addition of DDAB offers extra Br $^-$ ions and therefore suppresses the negative exciton trapping effects of surface halide vacancies [47]. However, the further increase of the ratio to 1:2 cause the PLQY dramatically decrease to 1.21%, which is accordance with the phenomenon on Figure S1b.

The time-resolved PL decay curves are shown in Fig. 1c, from which average PL decay times (τ_{ave}) of 23.60, 43.88, 39.81, and 23.87 ns can be obtained for the ratio values of 1:0, 1:0.25, 1:0.5 and 1:1, respectively. Compared with pure CsPbBr₃ QDs, the PL lifetimes of the DDAB-CsPbBr₃ ODs are relatively prolonged, indicating the successfully passivation of surface defects using DDAB. The radiative (k_{τ}) and nonradiative $(k_{n\tau})$ rate constants of these sample were then estimated from the PLQY value and average PL lifetimes according to ref [48]. As summarized in Table S1, the maximum k_{τ} value of DDAB-CsPbBr₃ QDs (3.0 × 10⁻²) increases by an order of magnitude compare with that in pure CsPbBr3 QDs (4.6 \times 10⁻³), which is in agreement with the growth trend of PLQY curves. In addition, the concentration of TMOS also affects the PLQY of QDs. When the concentration of TMOS is low, inorganic silica can cover the dangling bonds and defects exposed on the surface of QDs. However, the hydrolysis reaction needs long time and produces a small quantity of alcohol, When the concentration of TMOS is high, more water would be involved in the reaction and the quantity of by-product alcohol would increase, which might cause that the performance of QDs degrade, thus PLOY declines slightly. As confirmed by Fig. 1d. a highest PLOY of 82% is achieved with the adding of 5 μ L TMOS to coat the QDs, which is consistent with the observed phenomena under UV light (Fig. 1e).

To analyze the phase structures and composition of the QDs, X-ray diffraction (XRD) patterns and Fourier transform infrared spectroscopy (FTIR) were then performed. Fig. 2a shows the X-ray diffraction (XRD) patterns of pure CsPbBr₃ QDs, DDAB-CsPbBr₃ QDs (the molar ratio of Pb:DDAB = 1:1) and DDAB-CsPbBr₃/SiO₂ QDs composites (TOMS = 5 μ L). While CsPbBr₃ QDs exhibit diffraction peaks at 15.23°, 21.55°, 30.43°, 34.42°, 37.86° and 43.82°, which correspond to (100), (110), (200), (210), (211) and (202) planes of CsPbBr₃ QDs (PDF#18-0364), respectively. Similar diffraction peaks are found for both DDAB-CsPbBr₃ QDs and DDAB-CsPbBr₃/SiO₂ QDs composites, indicating that both the treatment with DDAB and coating with SiO₂ have a negligible influence on the crystalline. A broad peak is found at around 20° in the coated QDs, which is related to the formation of amorphous SiO₂ and is similar to silica-coated nanomaterials reported previously [49].

To further study it, Fourier Transform Infrared (FTIR) spectra of pure $CsPbBr_3$ QDs, DDAB- $CsPbBr_3$ QDs and DDAB- $CsPbBr_3/SiO_2$ QDs composites were measured, as shown in Fig. 2b. A peak at 3500 cm⁻¹ and a peak at around 1650 cm⁻¹ were found in the FTIR spectra of DDAB- $CsPbBr_3$ QDs and DDAB- $CsPbBr_3/SiO_2$ QDs composites, which may be due to the symmetric stretching of N-H and asymmetric NH³⁺

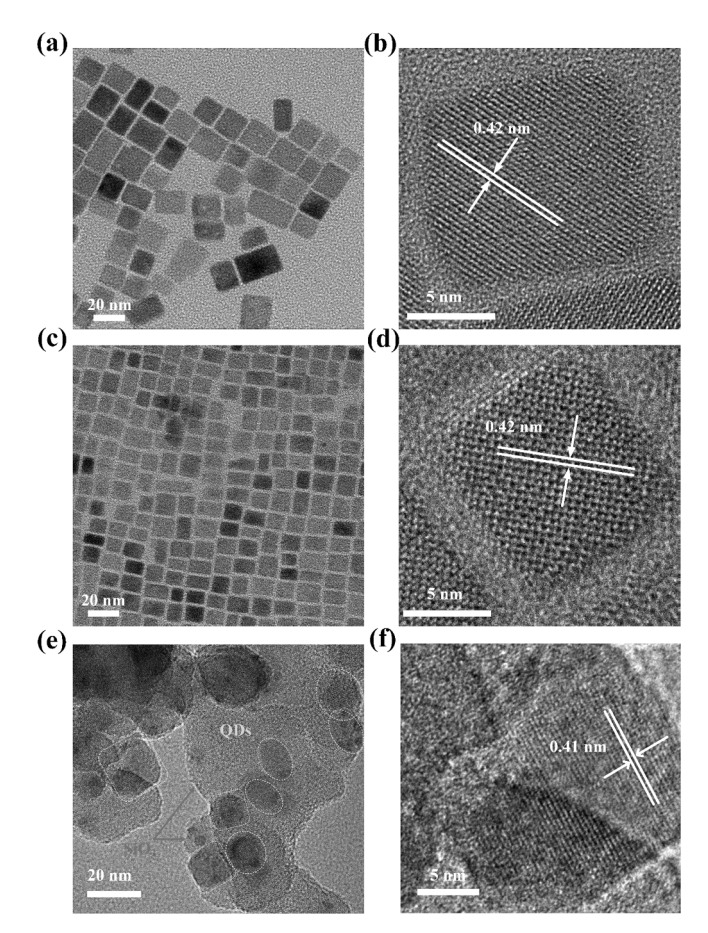


Fig. 3. TEM and HRTEM images of CsPbBr₃ QDs (a and b), DDAB-CsPbBr₃ QDs (c and d) and DDAB-CsPbBr₃/SiO₂ QDs composites (e and f).

deformation [50], respectively. A new peak assigned to the stretching modes of C-N⁺ of DDAB is found at 1070 cm⁻¹ in DDAB treated CsPbBr₃ QDs (Figure S2) [51], indicating the successful capping of DDAB on the surface of QDs. Besides, DDAB-CsPbBr₃/SiO₂ QDs composites show two additional strong peaks at 1050 cm⁻¹ and 795 cm⁻¹ compared with other two QDs, which correspond to Si–O–Si bonds and Si-OH bonds, respectively, demonstrating the successful coating with SiO₂. To further confirm this, X-ray photoelectron spectroscopy (XPS) measurement was performed to explore the surface chemical states, as shown in Figure S3. The presence of Cs, Pb, and Br elements is confirmed by the representative survey spectra of the three samples (Figure S3a). Figures S3b and

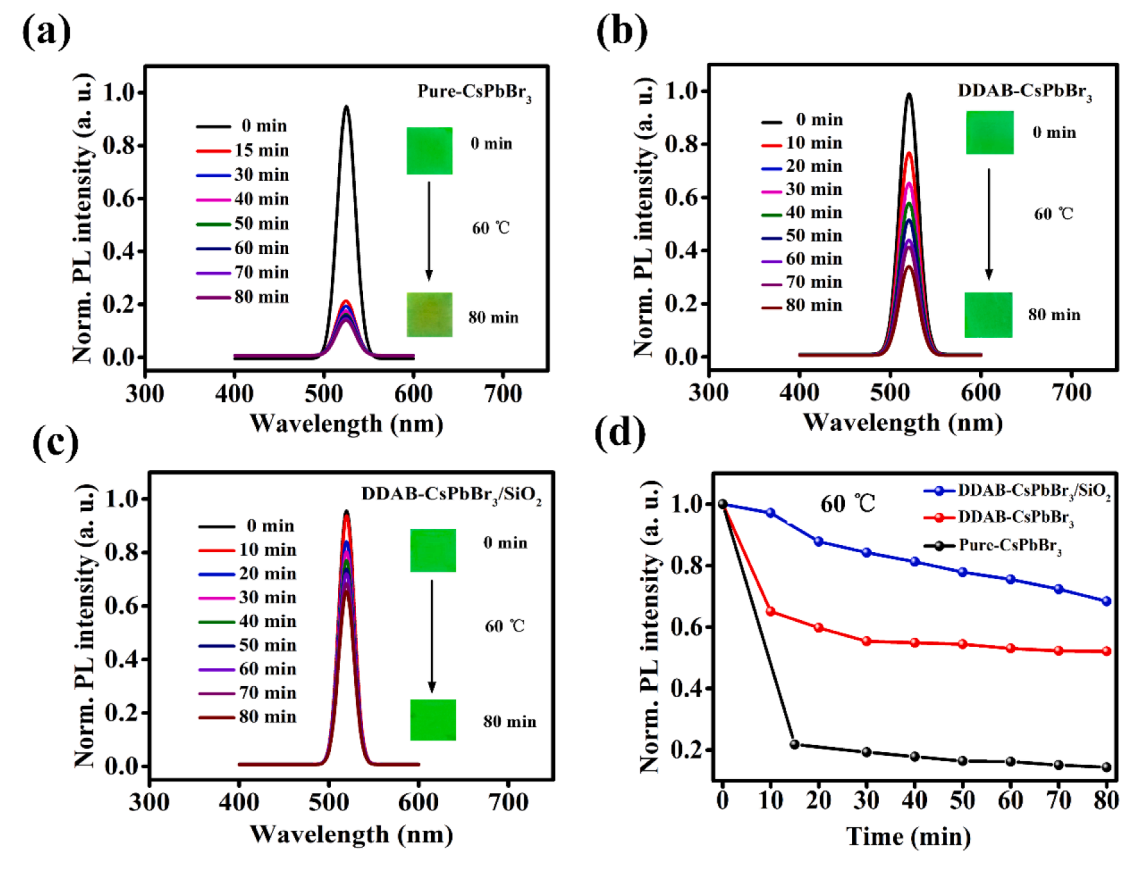


Fig. 4. PL spectra of (a) pure CsPbBr₃ QDs, (b) DDAB-CsPbBr₃ QDs and (c) DDAB-CsPbBr₃/SiO₂ QDs composites under a continuous heating at 60 °C with the insets showing photographs of the QD films under UV light) (d) The corresponding normalized PL intensity as a function of heating time.

S3c show the chemical states of Cs⁺ and Pb for all three QDs. The symmetric XPS peaks and the stable binding energy of three samples demonstrate a weak interaction (non-bonding states) between Cs⁺ and the [PbX₆]⁴⁻ octahedron [47]. After treating with DDAB, Pb 4*f* peak shifts slightly to a higher binding energy, which might be attributed to the bonding of surface Pb ions from CsPbBr₃ QDs with Br ions from DDAB [47,52]. Besides, the Si 2p peak (102.8 eV) and O 1s peak (531.8 eV) originate from SiO₂ could only be observed in the XPS curves of DDAB-CsPbBr₃/SiO₂ QDs composites, suggesting the successful coating of DDAB-CsPbBr₃ QDs surface with SiO₂.

To intuitively observe the microstructures of all three QDs, transmission electron microscopy (TEM) and high resolution TEM (HRTEM) were used to analyze their morphology features, as shown in Fig. 3. It is found that the shape of CsPbBr3 QDs undergoes no obvious change before and after the DDAB treatment, both presenting a cubic shape and monodisperse. Also, as shown in Fig. 3b and 3d, CsPbBr3 QDs treated with and without DDAB have same crystal lattices with a lattice spacing distance of 0.42 nm, which corresponds to the plane lattice spacing of (110). The coating of the QDs with silicon dioxide is confirmed distinctly by the TEM image in Fig. 3e, and the coated CsPbBr3 QDs exhibit a lattice spacing distance of 0.41 nm, as shown in Fig. 3f. Figure S4 shows the Energy-dispersive spectroscopy (EDS) elemental mapping of the DDAB-CsPbBr3/SiO2 QD composite films, from which a uniform distribution of Si and O elements in the selected square area is clearly seen, confirming the successful and uniform encapsulation of DDAB-CsPbBr3 QDs with silicon dioxide.

The instability of halide perovskites greatly hampers their practical applications in optoelectronic devices. To pursue whether the DDAB modification and silica capping improve the stability of CsPbBr₃, we here studied their chemical stability. As a comparison, the chemical stability of pure CsPbBr₃ QDs and DDAB-CsPbBr₃ QDs was also studied. First, the thermostability was examined by heating the QDs at different

temperature in a same ambient condition. As shown in Figure S5, QDs without coated by silica suffer a rapid fluorescence quenching, initially. In contrast, the PL intensity of silica-coated DDAB-CsPbBr3 QDs composites begins to decrease when annealing temperature reaches 60 °C and remains \sim 50% of its initial intensity at 100 °C. To further study heat resistance, The relative time-dependent PL curves of these QDs being heated at 60 °C in same ambient condition were studied. The change of the relative PL intensity alone with heating time for three ODs are shown in Fig. 4a-c. A rapid fluorescence quenching is found in the pure CsPbBr $_3$ film after being heated for 15 min and retains only $\sim 22\%$ of its initial intensity, mainly due to the falling of ligands (OA or OAm) from the surface of QDs and the additional structural defects caused by the heating. In contrast, the PL intensity of the DDAB-CsPbBr3 film experiences a relatively slower decrease and remains 52% of the initial intensity after being heated for 80 min, owing to the steric hindrance of DDA⁺ on the surface of the QDs [53]. A further increase of the PL intensity is found in DDAB-CsPbBr3/SiO2 film, which maintains approximately 70% of its initial intensity after being heated for 80 min, as shown in Fig. 4d, suggesting the effective passivation using SiO₂ shells.

Polar solvents, such as ethanol might easily damage QDs, leading to fluorescence quenching. To study it, we here tested the stability of our QDs against ethanol. While the PL intensity of pure CsPbBr $_3$ QDs and DDAB-CsPbBr $_3$ QDs maintain only 26% and 51% of their initial intensity, respectively, with the increase of ethanol amount from 0 to 250 μ L. DDAB-CsPbBr $_3$ /SiO $_2$. QDs composites remain a high PL intensity of 90% of their initial value, as shown in Figure S7. The relative time-dependent PL curves of these QDs after adding 200 μ L ethanol into 3 mL QDs solutions were also studied, as shown in Fig. 5a-c. Clearly, the PL intensity of pure CsPbBr $_3$ QDs quickly weaken and even almost quench within a short time of 30 min, in agreement with the photograph under UV light (Fig. 5a inset). Moreover, it is found that a new peak appears after 15 min, which might be related to the decomposition of

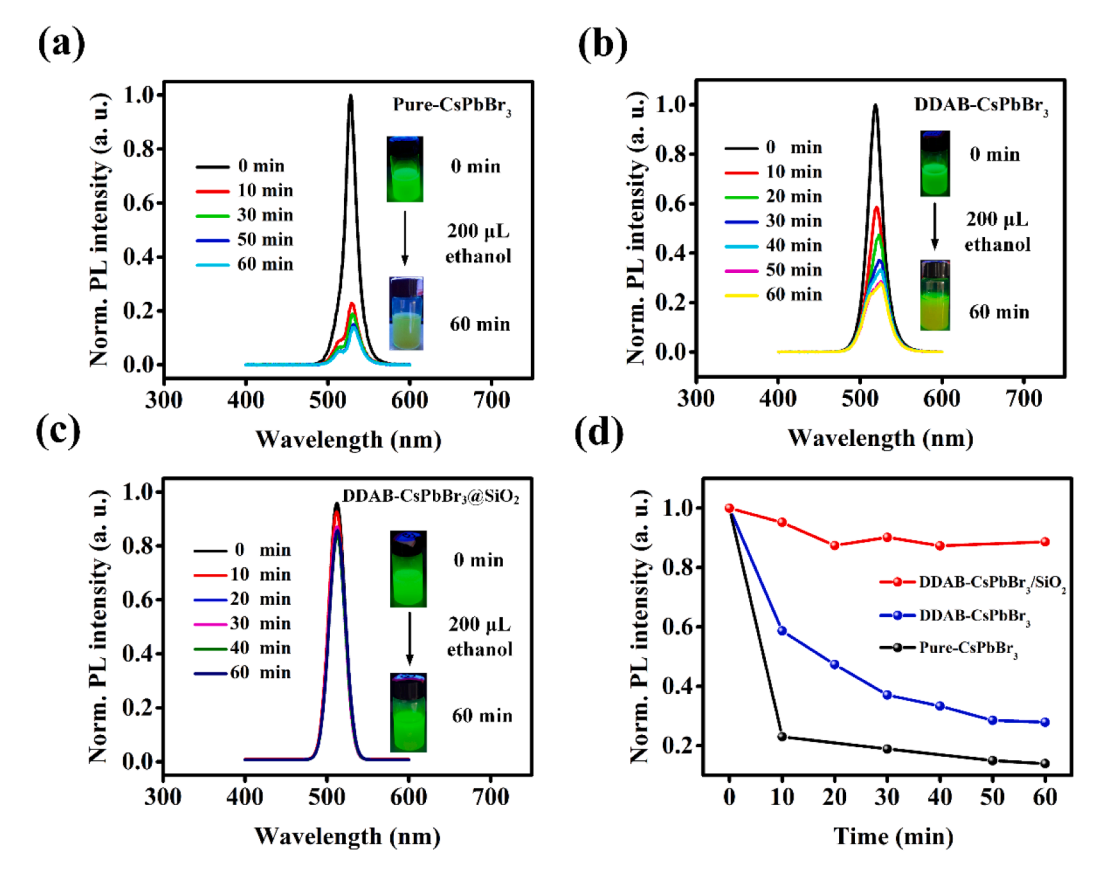


Fig. 5. PL spectra of (a) pure CsPbBr₃ QDs, (b) DDAB-CsPbBr₃ QDs and (c) DDAB-CsPbBr₃/SiO₂ QDs composites in ethanol. The insets show pictures of the QD solutions under UV light. (d) Normalized PL intensity as a function of treated time in ethanol.

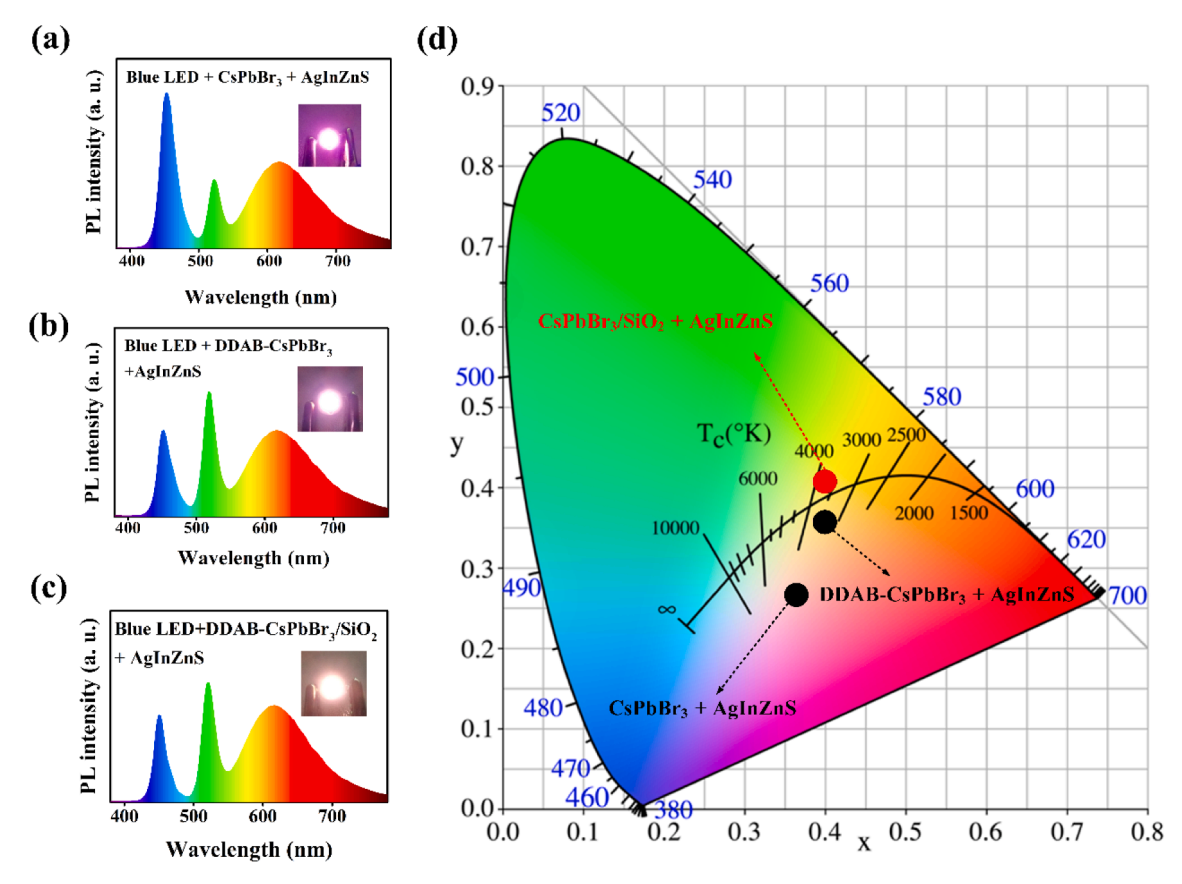


Fig. 6. PL spectra of WLEDs based on (a) pure $CsPbBr_3$ and AgInZnS QDs, (b) $DDAB-CsPbBr_3$ and AgInZnS QDs, and (c) $DDAB-CsPbBr_3/SiO_2$ and AgInZnS QDs. The insets show photographs of working WLEDs at a driving voltages of 2.6 V. (d) CIE color coordinates of all three WLEDs.

Table 1
Optical performance of WLEDs obtained by combining of blue chips, AgInZnS QDs and pure CsPbBr₃ or DDAB-CsPbBr₃ or DDAB-CsPbBr₃/SiO₂.

Samples	CCT (K)	CRI	Power efficiency (lm W^{-1})	CIE coordinates	
				x	у
Pure CsPbBr ₃ + AgInZnS	3592	72	20.1	0.36	0.27
DDAB-CsPbBr ₃ + AgInZnS	3629	84	41.8	0.39	0.36
DDAB-CsPbBr ₃ /SiO ₂ + AgInZnS	3209	88	63.4	0.41	0.38

CsPbBr3 QDs. Although the PL intensity of DDAB-CsPbBr3 QDs experience a relatively slower decrease compared with the pure CsPbBr₃ QDs case, still only 33% of their initial intensity remains after 60 min. In sharp contrast, DDAB-CsPbBr3/SiO2. QDs composites present a better tolerance to ethanol and maintain nearly 89% of their initial intensity even after 60 min. Such an improvement is considered mainly due to the effective silica- capping of DDAB-CsPbBr3 QDs, which defends the damage from ethanol. Moreover, considering that the application conditions of QDs are not in the vapor of ethanol but in water, the moisture stability of QDs is studied by adding 0.5 mL water into 2.5 mL CsPbBr₃, DDAB-CsPbBr3, and DDAB-CsPbBr3/SiO2, respectively. As shown in Figure S6, the rapid fluorescence quenching is found after 60 min and 30 min in the pure CsPbBr3 and DDAB-CsPbBr3, respectively. However, the PL intensity of the DDAB-CsPbBr3/SiO2 QDs composites remains 50% of the initial intensity after 210 min, which demonstrates SiO₂ shell can protect QDs from water effectively. All results suggest that the

chemical stability of CsPbBr₃ QDs has significantly enhanced by forming the silica coating layer on the DDAB-treated CsPbBr₃ QDs.

To demonstrate the potential of DDAB-CsPbBr₃/SiO₂ QDs composites as green-emitting components in commercialized warm white lighting source, AgInZnS QDs synthesized by a hot-injection synthesis strategy as the red-emitting component with pure CsPbBr₃ [54], DDAB-CsPbBr₃ and DDAB-CsPbBr₃/SiO₂ were dropped on InGaN blue chips to realize white emission, respectively. Fig. 6a-c present the PL spectra of WLEDs based on pure CsPbBr₃, DDAB-CsPbBr₃ and DDAB-CsPbBr₃/SiO₂ QDs composites at a driving voltage of 2.6 V, respectively. Fig. 6d shows that the CIE color coordinates of three WLEDs locate at (0.36, 0.27), (0.39, 0.36) and (0.41, 0.38), respectively. The PL intensity of DDAB-CsPbBr3 and DDAB-CsPbBr3/SiO2 QDs composites are higher than pure CsPbBr3 QDs, which might be the reason for the shift of color coordinates towards green region. Other key parameters of WLEDs including color rendering index (CRI), color temperature (CCT), and power efficiency are summarized in Table 1. Clearly, WLEDs based on SiO₂-coated DDAB-CsPbBr₃ QDs exhibit the best performance, including a CRI of 88 and a power efficiency of 63.4 lm W⁻¹. Such an enhanced performance as compared with their counterparts might be related to the higher PL intensity and the higher PLOY of DDAB-CsPbBr₃/SiO₂ QDs composites.

To further analyze the performance of three WLEDs, PL spectra of three WLEDs under different driving voltages (2.5–3.0 V) were studied, as shown in Figures S8-S10. The rise of chip temperature causes the thermal quenching effect of QDs, resulting in a slight shift of CIE coordinate towards red region. Meanwhile, the CRI of pure CsPbBr₃ based WLEDs is only 47 at 3.0 V, which is ascribed to the weaker thermal resistance (Table S2). A small change of CRI is found in both DDAB-

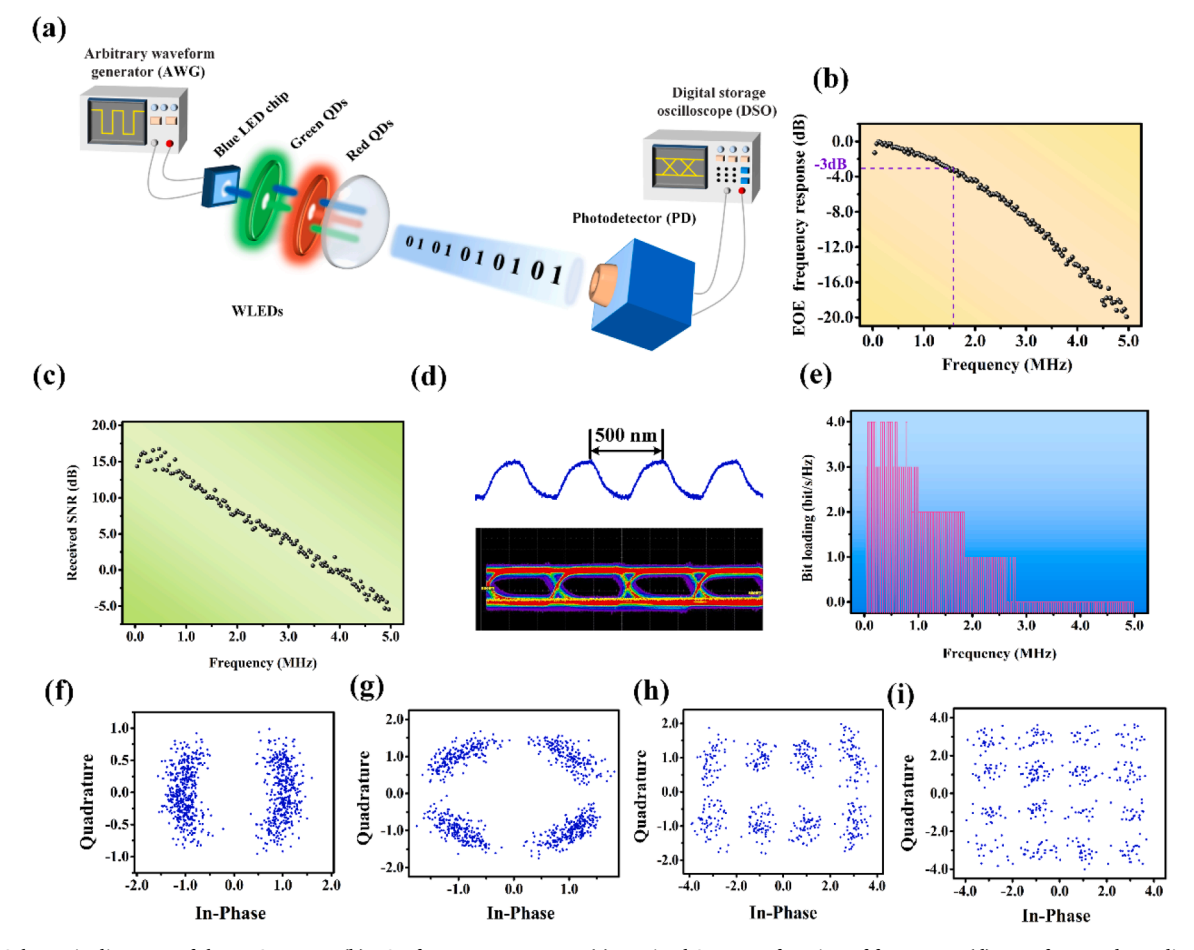


Fig. 7. (a) Schematic diagrams of the VLC system. (b) EOE frequency response, (c) received SNR as a function of frequency, (d) waveform and eye diagram, (e) bit loading profile. (f) BPSK constellation. (g) 4 QAM constellation, (h) 8 QAM constellation and (i) 16 QAM constellation

 $CsPbBr_3$ and $DDAB-CsPbBr_3/SiO_2$ based WLEDs, suggesting a better thermal stability of such materials. $DDAB-CsPbBr_3/SiO_2$ based WLEDs maintained a high CRI of 86 under a driving bias of 3 V while those based on $DDAB-CsPbBr_3$ show a CRI of only 73. (Tables S2 and S3), demonstrating that $DDAB-CsPbBr_3/SiO_2$ based WLEDs exhibit the best performance among all three types of WLEDs.

Besides lighting, WLEDs can also be used as optical sources to transmit data in VLC systems. Here, we studied the communication performance of WLEDs based on DDAB-CsPbBr3/SiO2 QDs composites using the measurement setup shown in Fig. 7a. Fig. 7b shows the electrical-optical-electrical (EOE) frequency response of the VLC system using such a WLED under a DC bias of 3.0 V. Clearly, the WLEDs exhibit a typical low-pass frequency response with a corresponding -3 dB bandwidth of about 1.5 MHz. The received signal-to-noise ratio (SNR) of the VLC system is shown in Fig. 7c, from which a gradually decrease of SNR with the increase of frequency is found. A typical square wave with a frequency of 2 MHz was then transmitted using such a WLED and Fig. 7d presents the measured waveform and eye diagram. Clear eyes can be obtained, indicating that DDAB-CsPbBr₃/SiO₂ based WLEDs are capable of working properly at a frequency of 2 MHz. In order to explore the maximum transmission data rate of such a WLED based VLC system, an orthogonal frequency division multiplexing (OFDM) with a bit loading was transmitted according to the measured SNR performance given in Fig. 7c. The obtained bit loading profile is shown in Fig. 7e and the received corresponding constellation diagrams, including binary phase shift keying (BPSK), 4-ary quadrature amplitude modulation (4 QAM), 8 QAM and 16 QAM, are plotted in Fig. 7f-i. By applying OFDM with a bit loading, the maximum achievable rate of 5.9 Mbps is found in the VLC system, which is approximately 4-fold of the measured -3 dB bandwidth.

4. Conclusions

In summary, this work demonstrates a facile and effective strategy to enhance the performance of CsPbBr3 QDs, which is done by first treating the QDs with DDAB and then coating them with SiO2. The reaction environment is fully at room-temperature and the cost is low, making it conducive to large-scale commercial productions. The obtained DDAB-CsPbBr₃/SiO₂ QDs composites illustrate a significantly enhanced PLQY and stability against ethanol and heat compared with their non-treated counterparts. The fabricated DDAB-CsPbBr3/SiO2 based WLEDs show an excellent luminescent performance with a CRI of 88, a color coordinate of (0.41, 0.38), a CCT of 3209 K and a power efficiency of 63.4 lm W⁻¹, demonstrating their broad future applications in solid-state lighting fields. WLEDs based on DDAB-CsPbBr3/SiO2 were also demonstrated in a VLC system and the results clearly suggested the potential of this highperformance WLEDs as an excitation light source to achieve visible light communication. As a result, the method and the prepared devices might have a great potential in future low-cost, high efficiency white lighting and visible light wireless communication field.

Declaration of Competing Interest

The authors claim that this manuscript has not been published in whole or in part nor is it being considered for publication elsewhere and declare no competing financial interest.

Acknowledgements

This work was financially supported by the Graduate Scientific Research and Innovation Foundation of Chongqing, China (CYS20064), National Natural Science Foundation of China (11974063, 61904023), Key Program Science Foundation of Natural Science Foundation of Chongqing (cstc2020jcyj-jqX0028), and Chongqing Special Postdoctoral Science Foundation (cstc2019jcyj-54bsh0026). The authors acknowledge Analytical and Testing Center of Chongqing University.

Appendix A. Supplementary data

Supplementary data to this article can be found online at https://doi.org/10.1016/j.cej.2021.129551.

References

- [1] Q.A. Akkerman, V. D'Innocenzo, S. Accornero, A. Scarpellini, A. Petrozza, M. Prato, L. Manna, Tuning the optical properties of cesium lead halide perovskite nanocrystals by anion exchange reactions, J. Am. Chem. Soc. 137 (32) (2015) 10276–10281.
- [2] X.X. He, P. Liu, H.H. Zhang, Q. Liao, J.N. Yao, H.B. Fu, Patterning multicolored microdisk laser arrays of cesium lead halide perovskite, Adv. Mater. 29 (2017) 8.
- [3] L. Lv, Y. Xu, H. Fang, W. Luo, F. Xu, L. Liu, B. Wang, X. Zhang, D. Yang, W. Hu, A. Dong, Generalized colloidal synthesis of high-quality, two-dimensional cesium lead halide perovskite nanosheets and their applications in photodetectors, Nanoscale 8 (28) (2016) 13589–13596.
- [4] P. Ramasamy, D.-H. Lim, B. Kim, S.-H. Lee, M.-S. Lee, J.-S. Lee, All-inorganic cesium lead halide perovskite nanocrystals for photodetector applications, Chem. Commun. 52 (10) (2016) 2067–2070.
- [5] J.H. Li, L.M. Xu, T. Wang, J.Z. Song, J.W. Chen, J. Xue, Y.H. Dong, B. Cai, Q. S. Shan, B.N. Han, H.B. Zeng, 50-Fold EQE improvement up to 6.27% of solution-processed all-inorganic perovskite CsPbBr₃ QLEDs via surface ligand density control, Adv. Mater. 29 (2017) 9.
- [6] G. Nedelcu, L. Protesescu, S. Yakunin, M.I. Bodnarchuk, M.J. Grotevent, M. V. Kovalenko, Fast anion-exchange in highly luminescent nanocrystals of cesium lead halide perovskites (CsPbX₃, X = Cl, Br, I), Nano lett. 15 (8) (2015) 5635–5640.
- [7] L. Protesescu, S. Yakunin, M.I. Bodnarchuk, F. Krieg, R. Caputo, C.H. Hendon, R. X. Yang, A. Walsh, M.V. Kovalenko, Nanocrystals of cesium lead halide perovskites (CsPbX₃, X = Cl, Br, and I): novel optoelectronic materials showing bright emission with wide color gamut, Nano lett. 15 (2015) 3692–3696.
- [8] S. Wei, Y. Yang, X. Kang, L. Wang, L. Huang, D. Pan, Room-temperature and gramscale synthesis of CsPbX₃ (X = Cl, Br, I) perovskite nanocrystals with 50–85% photoluminescence quantum yields, Chem. Commun. 52 (45) (2016) 7265–7268.
- [9] D. Zhang, Y. Yang, Y. Bekenstein, Y.i. Yu, N.A. Gibson, A.B. Wong, S.W. Eaton, N. Kornienko, Q. Kong, M. Lai, A.P. Alivisatos, S.R. Leone, P. Yang, Synthesis of composition tunable and highly luminescent cesium lead halide nanowires through anion-exchange reactions, J. Am. Chem. Soc. 138 (23) (2016) 7236–7239.
- [10] H. Hu, L. Wu, Y. Tan, Q. Zhong, M. Chen, Y. Qiu, D.i. Yang, B. Sun, Q. Zhang, Y. Yin, Interfacial synthesis of highly stable CsPbX₃/oxide Janus nanoparticles, J. Am. Chem. Soc. 140 (1) (2018) 406–412.
- [11] Z. Li, L. Kong, S. Huang, L. Li, Highly luminescent and ultrastable CsPbBr₃ perovskite quantum dots incorporated into a silica/alumina monolith, Angew. Chem. Int. Edit. 56 (28) (2017) 8134–8138.
- [12] J. Pan, Y. Shang, J. Yin, M. De Bastiani, W. Peng, I. Dursun, L. Sinatra, A.M. El-Zohry, M.N. Hedhili, A.-H. Emwas, O.F. Mohammed, Z. Ning, O.M. Bakr, Bidentate ligand-passivated CsPbI₃ perovskite nanocrystals for stable near-unity photoluminescence quantum yield and efficient red light-emitting diodes, J. Am. Chem. Soc. 140 (2) (2018) 562–565.
- [13] Z. Liu, Y. Zhang, Y.i. Fan, Z. Chen, Z. Tang, J. Zhao, Y. Iv, J. Lin, X. Guo, J. Zhang, X. Liu, Toward highly luminescent and stabilized silica-coated perovskite quantum dots through simply mixing and stirring under room temperature in Air, ACS Appl. Mater. Interfaces 10 (15) (2018) 13053–13061.
- [14] M.V. Kovalenko, L. Protesescu, M.I. Bodnarchuk, Properties and potential optoelectronic applications of lead halide perovskite nanocrystals, Science 358 (6364) (2017) 745–750.
- [15] S. Zhao, Y. Zhang, Z. Zang, Room-temperature doping of ytterbium into efficient near-infrared emission CsPbBr_{1.5}Cl_{1.5} perovskite quantum dots, Chem. Commun. 56 (2020) 5811–5814.
- [16] X. Li, Y. Wu, S. Zhang, B. Cai, Y. Gu, J. Song, H. Zeng, CsPbX₃ Quantum dots for lighting and displays: room-temperature synthesis, photoluminescence superiorities, underlying origins and white light-emitting diodes, Adv. Funct. Mater. 26 (2016) 2435–2445.
- [17] Y.u. Cao, N. Wang, H.e. Tian, J. Guo, Y. Wei, H. Chen, Y. Miao, W. Zou, K. Pan, Y. He, H. Cao, Y. Ke, M. Xu, Y. Wang, M. Yang, K. Du, Z. Fu, D. Kong, D. Dai, Y. Jin, G. Li, H. Li, Q. Peng, J. Wang, W. Huang, Perovskite light-emitting diodes based on spontaneously formed submicrometre-scale structures, Nature 562 (7726) (2018) 249-253
- [18] T. Leijtens, G.E. Eperon, N.K. Noel, S.N. Habisreutinger, A. Petrozza, H.J. Snaith, Stability of metal halide perovskite solar cells, Adv. Energy Mater. 5 (2015) 23.
- [19] J. Song, J. Li, X. Li, L. Xu, Y. Dong, H. Zeng, Quantum dot light-emitting diodes based on inorganic perovskite cesium lead halides (CsPbX₃), Adv. Mater. 27 (44) (2015) 7162–7167.
- [20] G. Li, F.W.R. Rivarola, N.J.L.K. Davis, S. Bai, T.C. Jellicoe, F. de la Peña, S. Hou, C. Ducati, F. Gao, R.H. Friend, N.C. Greenham, Z.-K. Tan, Highly efficient perovskite nanocrystal light-emitting diodes enabled by a universal crosslinking method, Adv. Mater. 28 (18) (2016) 3528–3534.
- [21] K.-H. Wang, L. Wu, L. Li, H.-B. Yao, H.-S. Qian, S.-H. Yu, Large-Scale synthesis of highly luminescent perovskite-related CsPb₂Br₅ nanoplatelets and their fast anion exchange, Angew. Chem. Int. Edit. 55 (29) (2016) 8328–8332.
- [22] M. Chen, Y. Zou, L. Wu, Q.i. Pan, D.i. Yang, H. Hu, Y. Tan, Q. Zhong, Y. Xu, H. Liu, B. Sun, Q. Zhang, Solvothermal synthesis of high-quality all-inorganic cesium lead halide perovskite nanocrystals: from nanocube to ultrathin nanowire, Adv. Funct.

- Mater. 27 (23) (2017) 1701121, https://doi.org/10.1002/adfm.v27.2310.1002/adfm.201701121.
- [23] L. Wu, H. Hu, Y. Xu, S. Jiang, M. Chen, Q. Zhong, D. Yang, Q. Liu, Y. Zhao, B. Sun, Q. Zhang, Y. Yin, From nonluminescent Cs₄PbX₆ (X = Cl, Br, I) Nanocrystals to highly luminescent CsPbX₃ nanocrystals: water-triggered transformation through a CsX-stripping mechanism, Nano Lett. 17 (2017) 5799–5804.
- [24] H. Zhou, S. Yuan, X. Wang, T. Xu, X. Wang, H. Li, W. Zheng, P. Fan, Y. Li, L. Sun, A. Pan, Vapor growth and tunable lasing of band gap engineered cesium lead halide perovskite micro/nanorods with triangular cross section, ACS Nano 11 (2) (2017) 1189–1195.
- [25] J. Pan, L.N. Quan, Y. Zhao, W. Peng, B. Murali, S.P. Sarmah, M. Yuan, L. Sinatra, N. M. Alyami, J. Liu, E. Yassitepe, Z. Yang, O. Voznyy, R. Comin, M.N. Hedhili, O. F. Mohammed, Z.H. Lu, D.H. Kim, E.H. Sargent, O.M. Bakr, Highly efficient perovskite-quantum-dot light-emitting diodes by surface engineering, Adv. Mater. 28 (39) (2016) 8718–8725.
- [26] Y. Tan, Y. Zou, L. Wu, Q.i. Huang, D.i. Yang, M. Chen, M. Ban, C. Wu, T. Wu, S. Bai, T. Song, Q. Zhang, B. Sun, Highly luminescent and stable perovskite nanocrystals with octylphosphonic acid as a ligand for efficient light-emitting diodes, ACS Appl. Mater. Interfaces 10 (4) (2018) 3784–3792.
- [27] M. Imran, P. Ijaz, L. Goldoni, D. Maggioni, U. Petralanda, M. Prato, G. Almeida, I. Infante, L. Manna, Simultaneous cationic and anionic ligand exchange For colloidally stable CsPbBr₃ nanocrystals, ACS Energy Lett. 4 (4) (2019) 819–824.
- [28] D. Yan, T. Shi, Z. Zang, T. Zhou, Z. Liu, Z. Zhang, J. Du, Y. Leng, X. Tang, Ultrastable CsPbBr₃ perovskite quantum dot and their enhanced amplified spontaneous emission by surface ligand modification, Small 15 (2019) 1901173.
- [29] D. Yang, X. Li, W. Zhou, S. Zhang, C. Meng, Y. Wu, Y. Wang, H. Zeng, CsPbBr₃ quantum dots 2.0: benzenesulfonic acid equivalent ligand awakens complete purification, Adv. Mater. 31 (2019) 1900767.
- [30] D. Yan, T. Shi, Z. Zang, S. Zhao, J. Du, Y. Leng, Stable and low-threshold whispering-gallery-mode lasing from modified CsPbBr₃ perovskite quantum dots@ SiO₂ sphere, Chem. Eng. J. 401 (2020), 126066.
- [31] D. Yan, S. Zhao, H. Wang, Z. Zang, Ultrapure and highly efficient green light emitting devices based on ligand-modified CsPbBr₃ quantum dots, Photonics Res. 8 (7) (2020) 1086, https://doi.org/10.1364/PRJ.391703.
- [32] J.T. DuBose, P.V. Kamat, Surface chemistry matters. How ligands influence excited state interactions between CsPbBr₃ and methyl viologen, J. Phys. Chem. C 124 (24) (2020) 12990–12998.
- [33] L. Zhu, C. Wu, S. Riaz, J. Dai, Stable silica coated DDAB-CsPbX₃ quantum dots and their application for white light-emitting diodes, J. Lumin. 233 (2021), 117884.
- [34] Q. Zhang, I. Lee, J. Ge, F. Zaera, Y. Yin, Surface-protected etching of mesoporous oxide shells for the stabilization of metal nanocatalysts, Adv. Funct. Mater. 20 (14) (2010) 2201–2214.
- [35] Q. Zhang, I. Lee, J.B. Joo, F. Zaera, Y. Yin, Core-shell nanostructured catalysts, Acc. Chem. Res 46 (8) (2013) 1816–1824.
- [36] H.-C. Wang, S.-Y. Lin, A.-C. Tang, B.P. Singh, H.-C. Tong, C.-Y. Chen, Y.-C. Lee, T.-L. Tsai, R.-S. Liu, Mesoporous silica particles integrated with all-inorganic CsPbBr₃ perovskite quantum-dot nanocomposites (MP-PQDs) with high stability and wide color gamut used for backlight display, Angew. Chem. Int. Edit. 55 (28) (2016) 7924–7929.
- [37] D.Q. Chen, G.L. Fang, X. Chen, Silica-coated Mn-doped CsPb(Cl/Br)₃ inorganic perovskite quantum dots: exciton-to-Mn energy transfer and blue-excitable solidstate lighting, ACS Appl. Mater. Interfaces 9 (2017) 40477–40487.
- [38] L. Xu, J. Chen, J. Song, J. Li, J. Xue, Y. Dong, B.o. Cai, Q. Shan, B. Han, H. Zeng, Double-protected all-inorganic perovskite nanocrystals by crystalline matrix and

- silica for triple-modal anti-counterfeiting codes, ACS Appl. Mater. Interfaces 9 (31) (2017) 26556-26564.
- [39] Q. Mo, T. Shi, W. Cai, S. Zhao, D. Yan, J. Du, Z. Zang, Room temperature synthesis of stable silica-coated CsPbBr₃ quantum dots for amplified spontaneous emission, Photonics Res. 8 (10) (2020) 1605, https://doi.org/10.1364/PRJ.399845.
- [40] Z.J. Li, E. Hofman, J. Li, A.H. Davis, C.H. Tung, L.Z. Wu, W.W. Zheng, Photoelectrochemically active and environmentally stable CsPbBr₃/TiO₂Core/ Shell nanocrystals, Adv. Funct. Mater. 28 (2018) 7.
- [41] A. Loiudice, S. Saris, E. Oveisi, D.T.L. Alexander, R. Buonsanti, CsPbBr₃ QD/AlOx inorganic nanocomposites with exceptional stability in water, light, and heat, Angew. Chem. Int. Edit. 56 (36) (2017) 10696–10701.
- [42] J. Liu, L. Zhang, Q. Yang, C. Li, Structural control of mesoporous silicas with large nanopores in a mild buffer solution, Microporous Mesoporous Mater. 116 (1-3) (2008) 330–338.
- [43] S. Huang, Z. Li, L. Kong, N. Zhu, A. Shan, L. Li, Enhancing the stability of CH₃NH₃PbBr₃ quantum dots by embedding in silica spheres derived from tetramethyl orthosilicate in "Waterless" toluene, J. Am. Chem. Soc. 138 (18) (2016) 5749–5752.
- [44] H. Shao, X. Bai, G. Pan, H. Cui, J. Zhu, Y. Zhai, J. Liu, B. Dong, L. Xu, H. Song, Highly efficient and stable blue-emitting CsPbBr(3)@SiO(2) nanospheres through low temperature synthesis for nanoprinting and WLED, Nanotechnology 29 (2018), 285706.
- [45] Q. Zhong, M. Cao, H. Hu, D.i. Yang, M. Chen, P. Li, L. Wu, Q. Zhang, One-pot synthesis of highly stable CsPbBr₃@SiO₂ core-shell nanoparticles, ACS Nano 12 (8) (2018) 8579–8587.
- [46] X. Tang, W. Chen, Z. Liu, J. Du, Z. Yao, Y. Huang, C. Chen, Z. Yang, T. Shi, W. Hu, Z. Zang, Y. Chen, Y. Leng, Ultrathin, core-shell structured SiO₂ coated Mn²⁺-doped perovskite quantum dots for bright white light-emitting diodes, Small 15 (2019) 1900484
- [47] D.D. Yang, X.M. Li, Y. Wu, C.T. Wei, Z.Y. Qin, C.F. Zhang, Z.G. Sun, Y.L. Li, Y. Wang, H.B. Zeng, Surface halogen compensation for robust performance enhancements of CsPbX₃ perovskite quantum dots, Adv. Opt. Mater. 7 (2019) 10.
- [48] N. Mondal, A. De, A. Samanta, Achieving near-unity photoluminescence efficiency for blue-violet-emitting perovskite nanocrystals, ACS Energy Lett. 4 (1) (2019) 32–39.
- [49] C. Sun, Y.u. Zhang, C. Ruan, C. Yin, X. Wang, Y. Wang, W.W. Yu, Efficient and stable white leds with silica-coated inorganic perovskite quantum dots, Adv. Mater. 28 (45) (2016) 10088–10094.
- [50] L.D. White, C.P. Tripp, Reaction of (3-Aminopropyl)dimethylethoxysilane with amine catalysts on silica surfaces, J. Colloid Interface Sci. 232 (2) (2000) 400–407.
- [51] L. Zhang, X. Sun, Y. Song, X. Jiang, S. Dong, E. Wang, Didodecyldimethylammonium bromide lipid bilayer-protected gold nanoparticles: synthesis characterization, and self-assembly, Langmuir 22 (2006) 2838–2843.
- [52] J.Y. Woo, Y. Kim, J. Bae, T.G. Kim, J.W. Kim, D.C. Lee, S. Jeong, Highly stable cesium lead halide perovskite nanocrystals through in situ lead halide inorganic passivation, Chem. Mater. 29 (17) (2017) 7088–7092.
- [53] C. Zheng, C. Bi, F. Huang, D. Binks, J. Tian, Stable and strong emission CsPbBr 3 quantum dots by surface engineering for high-performance optoelectronic films, ACS Appl. Mater. Interfaces 11 (28) (2019) 25410–25416.
- [54] H.L. Guan, S.Y. Zhao, H.X. Wang, D.D. Yan, M. Wang, Z.G. Zang, Room temperature synthesis of stable single silica-coated CsPbBr 3 quantum dots combining tunable red emission of Ag-In-Zn-S for High-CRI white light-emitting diodes, Nano Energy 67 (2020) 9.